AJR FOCUS ON:

Biomechanical Investigation of the Classic Metaphyseal Lesion Using an Immature Porcine Model

Angela Thompson[1]
Gina Bertocci[2,3]
Kim Kaczor[4]
Craig Smalley[2]
Mary Clyde Pierce[4]

OBJECTIVE. The classic metaphyseal lesion is highly associated with abuse in infants. Classic metaphyseal lesions, also referred to as corner or bucket-handle fractures, are fractures through the metaphyseal region of the long bones near the growth plate. Knowledge of the biomechanics and mechanisms necessary to produce a classic metaphyseal lesion may provide insight into the injury causation associated with this unique fracture type. Thus, the purpose of this study was to investigate loading conditions necessary to create a classic metaphyseal lesion using an immature porcine model.

MATERIALS AND METHODS. Twenty-four pelvic limb specimens from 7-day-old and 3-day-old piglets were tested in lateral bending (varus and valgus) using an electromechanical testing machine. All specimens were loaded dynamically in four-point bending at a rate of 100 inches/min. Microcomputed tomography was performed on specimens before and after testing. Pre- and posttest CT images were compared to assess whether fracture had occurred.

RESULTS. Fractures resembling classic metaphyseal lesions were identified in 12 of the 24 specimens. Microcomputed tomography images revealed trabecular disruptions visually similar to classic metaphyseal lesions in children.

CONCLUSION. Metaphyseal fractures, consistent with clinical classic metaphyseal lesions, resulted from a single loading event delivering varus or valgus bending to the stifle (knee). A classic metaphyseal lesion is a unique type of fracture with specific morphologic characteristics. Therefore, we suggest using the term "classic metaphyseal fracture" in lieu of classic metaphyseal lesion to improve precision of terminology.

Keywords: biomechanics, child abuse, classic metaphyseal lesion, microcomputed tomography, pediatric fracture

DOI:10.2214/AJR.14.13267

Received June 6, 2014; accepted without revision July 28, 2014.

Supported by grant 2009-DD-BX-0086 (PI: G. Bertocci) awarded by the Office of Juvenile Justice and Delinquency Prevention, Office of Justice Programs, U.S. Department of Justice, and the Whitaker Foundation (PI: M. Pierce). Points of view or opinions expressed in this article are those of the authors and do not necessarily represent the official position or policies of the U.S. Department of Justice or the Whitaker Foundation.

[1]Department of Engineering Fundamentals, University of Louisville, Louisville, KY.

[2]Department of Bioengineering, University of Louisville, Louisville, KY.

[3]Department of Pediatrics, University of Louisville, Louisville, KY.

[4]Ann & Robert H. Lurie Children's Hospital, Northwestern University Feinberg School of Medicine, 225 E. Chicago Ave, Box 62, Chicago, IL 60611-2605. Address correspondence to M. C. Pierce (mpierce@luriechildrens.org).

WEB
This is a web exclusive article.

AJR 2015; 204:W503–W509

0361–803X/15/2045–W503

The classic metaphyseal lesion is highly associated with abuse in infants. In fatally abused infants, classic metaphyseal lesions are the most common fracture [1]. In a study of 31 fatally abused infants with skeletal injuries, Kleinman et al. [1] identified 64 classic metaphyseal lesions in 20 infants. A further study confirmed classic metaphyseal lesions to be the most common fracture type, with 40% of 89 total fractures occurring in 36 abused children being classic metaphyseal lesions [2]. Classic metaphyseal lesions most commonly occur at the distal femur and proximal tibia [3]. Classic metaphyseal lesions of the distal femur and proximal tibia often involve the medial aspect of the knee and extend to the lateral aspect in more severe cases [4, 5]. Aside from abusive trauma, classic metaphyseal lesions have otherwise been reported only as a result of birth trauma and treatment of clubfoot [6, 7].

Classic metaphyseal lesions, also referred to as corner or bucket-handle fractures, are fractures through the immature metaphyseal bone near the growth plate. Classic metaphyseal lesions are most commonly diagnosed using plain radiographs and may vary in appearance depending on several factors including the angle of the radiographic projection, time elapsed since injury, and extent of the fracture [7]. When the radiographic projection is perpendicular to the long axis of the bone, classic metaphyseal lesions often appear as a corner fracture; when the projection is nonperpendicular relative to the long axis of the bone, a bucket-handle pattern often appears [3]. Despite the differing appearance, classic metaphyseal lesions are planar fractures that may extend partially or completely through the metaphyseal bone and undercut the subperiosteal bone collar at the periphery [3].

Currently, the biomechanics associated with and loading conditions necessary to generate classic metaphyseal lesions are unknown. It has been suggested that shearing or tensile forces due to pulling an infant's

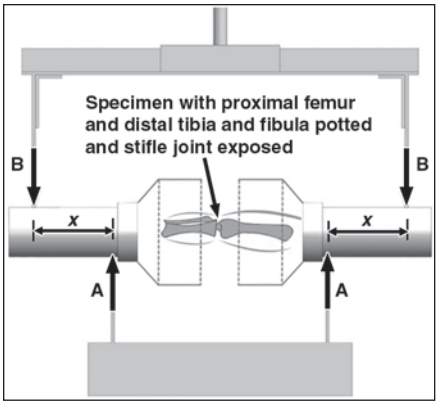

Fig. 1—Diagram shows immature porcine pelvic limb specimen positioned in electromechanical testing machine in custom four-point bending apparatus. Though not depicted, specimen was tested with soft tissue intact. Arrows indicate location and direction of force application, and "*x*" indicates distance between supports (A) and fixture components (B) applying downward load.

extremity, torsional loading associated with twisting an infant's extremity, or flailing of a victim's extremity during violent shaking may be the cause of these injuries [3, 7]. Several studies have attempted to produce classic metaphyseal lesion fractures using an immature porcine model. Ruess et al. [8] twisted the extremities of or shook eight cadaveric immature pigs; 68 metaphyseal fractures, consistent with classic metaphyseal lesions, were identified histologically and 22 through film-screen radiography. However, specific loading conditions (magnitude and direction of the applied forces) were not reported. Kleinman et al. [9] and O'Connor et al. [10] manually applied varus and valgus bending loads to the extremities of fetal pigs, generating classic metaphyseal lesions for the purpose of comparing film-screen radiography to computed radiography in identification of classic metaphyseal lesions. Again, details regarding the bending loading conditions were not reported.

Thus, the aim of the present study was to experimentally generate a classic metaphyseal lesion–type fracture in an immature porcine model and determine loading conditions (magnitude and direction of applied forces and moments) necessary to create the fracture. This was accomplished by controlled loading of immature porcine pelvic limb specimens. Because classic metaphyseal lesions are highly associated with abuse, knowledge of mechanisms needed to produce a classic metaphyseal lesion–type fracture in an immature animal model may advance our understanding of loading conditions that an infant is exposed to in order to generate a classic metaphyseal lesion.

Materials and Methods

In an attempt to produce a classic metaphyseal lesion experimentally in an animal model, immature porcine pelvic limb specimens were tested in lateral varus and valgus bending by using an electromechanical testing machine (eXpert 2610, ADMET). Lateral bending was chosen as the loading condition on the basis of previously reported success in generating fractures similar to classic metaphyseal lesions by using lateral (varus and valgus) bending [9].

Pelvic limb specimens of 3- and 7-day-old piglets ranging in weight from 1.7 to 2.8 kg (3-day-old) and 2.6–3.9 kg (7-day-old) were tested following an IACUC-approved protocol (IACUC protocol 10154). Previous studies have used immature pigs as a model for infants to investigate body composition [11–13], relationships between bone density measures acquired by dual-energy x-ray absorptiometry and bone strength [14, 15], fracture patterns [16, 17], and classic metaphyseal lesions [8–10]. To replicate the skeletal structure of infant extremities, we selected 3- and 7-day-old piglets because the 3- and 7-day-old porcine stifle (knee) joints were comparable to those of 3- to 9-month-old infants [18] with regards to ossification and metaphyseal and epiphyseal morphology.

Specimen Preparation

Specimens were preserved in saline-soaked gauze and stored frozen at –20°C until testing. Before testing, specimens were thawed to room temperature. Specimens were disarticulated at the tarsus (ankle joint) and hip, leaving the stifle (knee) joint and all associated bones (femur, tibia, fibula) and soft tissue intact. The skin was removed to prevent slippage in the testing apparatus. Two holes (0.078 inches [2.0 mm] in diameter) were drilled in the proximal femur and distal tibia, and 1.5-inch (38-mm)–long pins were inserted to secure the bone in the potting material. The stifle joint was fully extended, and the ends of the limbs were potted in automotive body filler, leaving the stifle joint unconstrained. The potted limbs were allowed to set for 30 minutes to ensure complete hardening of the body filler. Specimens were then secured in a custom four-point bending fixture and positioned for testing by use of an electromechanical testing machine (eXpert 2610, ADMET) (Fig. 1). The specimen was oriented so that the load was applied to either the medial or the lateral aspect of the pelvic limb, creating a varus or valgus bending moment, respectively. Inboard fixture supports (labeled "A" in Fig. 1 and positioned beneath the potted specimen) were fixed at an equal distance from fixture components applying downward loading (labeled "B" in Fig. 1), and the distance (*x* in Fig. 1) between inboard supports and fixture components was measured.

Mechanical Testing

Preliminary tests were performed on two specimens (one 3-day-old piglet and one 7-day-old piglet) to estimate the magnitude of failure (fracture) loads and determine the associated failure mechanism (fracture type and bone region of failure). The electromechanical testing machine was equipped with a 1000-lbf (4448-N) load cell (SM-1000, Interface). Specimens were loaded in four-point valgus bending at a rate of 100 inches/min (42.3 mm/s) and set to cutoff after a 20% reduction in measured force, indicating tissue failure and likely fracture. Force and displacement were sampled at 90 Hz. All tests were videotaped at 30 Hz. Bending moments, *M,* were calculated using the equation $M = (F/2)x$, where F is the force recorded by the load cell and x is the distance measured between fixture supports and fixture components (A and B, respectively, in Fig. 1). After preliminary tests, moment-versus-time data and videos were reviewed to determine point of failure and

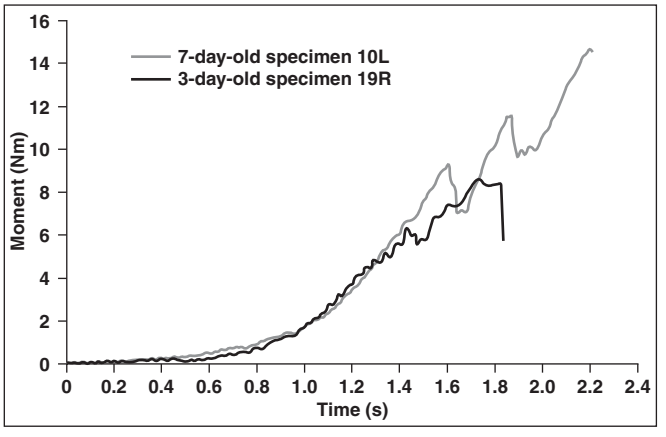

Fig. 2—Bending-moment-versus-time-curve shows loading applied to preliminary test specimens to estimate failure (fracture) loads. Sudden decreases in bending moment (drops in moment on time-history plots) are indicative of inability of pelvic limb to sustain continued loading because of tissue failure. Complete growth plate separation was failure mechanism in both specimens.

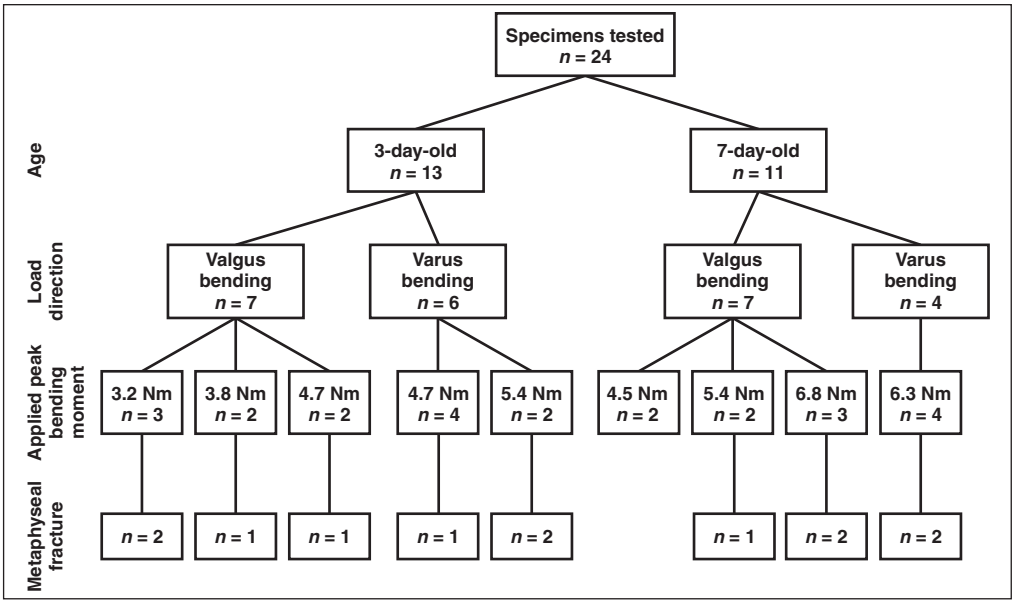

Fig. 3—Flow diagram for bending tests of porcine pelvic limb specimens shows specimen age, number of specimens tested under varus or valgus loading conditions, peak applied bending moment, and number of specimens with fracture(s) (total *n* = 12) based on microcomputed tomography.

failure loads. Specimens were dissected to assess failure mechanism. These tests revealed that tissue failure occurred at the femoral growth plate with complete separation of the cartilage from the metaphysis. Because classic metaphyseal lesions were expected to occur at loads less than the determined growth plate failure load, remaining tests of 3- and 7-day-old specimens (*n* = 24) were conducted with peak loads set at 50–85% of the growth plate failure load (from preliminary tests). Groupings of specimens were tested at various peak bending moments within the 50–85% of growth plate failure range to investigate whether loading within this range was capable of generating a classic metaphyseal lesion or whether a different failure mechanism would emerge. All specimens were dynamically loaded at a rate of 100 inches/min (42.3 mm/s) to replicate injury-causing scenarios. Testing ended when the bending moment reached the preset peak load. Statistical analysis was not performed given the small sample size.

Imaging

To identify whether a classic metaphyseal lesion occurred, we performed microcomputed tomography (Microphotonics; and Skyscan 1173, Bruker) on specimens before and after testing. All scans were conducted to achieve 20-μm resolution. Pre- and posttest images were reconstructed in Mimics image-processing software (version 15.0, Materialise) to view the specimens in 3D. Sagittal, coronal, and transverse views were compared to assess whether fracture had occurred. A classic metaphyseal lesion–type fracture was suspected if trabecular damage just proximal to the femoral growth plate or just to the tibial growth plate was identified on the posttest CT scan but not present on the pretest scan.

Results

Preliminary tests of 3- and 7-day-old specimens revealed that failure occurred at the femoral growth plate (complete separation of metaphyseal bone from cartilage). Review of the loading time-history plots (Fig. 2) revealed rapid drops or decreases in the bending moment, suggesting that tissue failure occurred. However, in general, rapid decreases in bending moment identified in time-history plots are not able to predict which tissue failed (soft tissue vs bone) or where the failure occurred. In our preliminary testing, the bending moment measured before the first substantial drop (Fig. 2; 6.3 Nm [56 inches × lbf] for 3-day-old specimen and 9.0 Nm [80 inches × lbf] for 7-day-old specimen) was used as the threshold below which all further testing would be conducted. This was chosen as a conservative estimate of growth plate failure load because classic metaphyseal lesions were expected to occur before growth plate failure.

Excluding the preliminary tests to determine failure loads, we tested 24 pelvic limb specimens (Fig. 3). Five specimens did not undergo posttest scanning and thus were excluded from further analysis: for one specimen, an error in the test setup occurred such that loading was not applied properly; three specimens had complete failure or separation of the femoral growth plate; and one specimen fractured at the location of the retention pin in the proximal femur. On the basis of the microcomputed tomography images, fracture patterns consistent with classic metaphyseal lesions were identified in 12 (five 7- and seven 3-day-old) specimens. These fracture patterns were identified in both loading directions (varus and valgus) and occurred within peak applied bending moments of 3.2–5.4 Nm in the 3-day-old specimens and 5.4–6.8 Nm in the 7-day-old specimens.

In the 12 specimens with fracture patterns consistent with classic metaphyseal lesions, fractures were identified at the distal femur in all specimens (*n* = 12) and at the proximal tibia in five specimens, yielding 17 fractures in total. Thus, five pelvic limb specimens had both femoral and tibial classic metaphyseal lesions. Microcomputed tomography images revealed that fractures generally appeared as a thin white line slightly distal to the femoral (or proximal to the tibial) metaphyseal surface (Figs. 4–6), indicating that mineralized bone tissue had separated from the metaphyseal body. The severity and extent of the fracture varied. Eight of the 17 fractures traversed the entire metaphysis (Fig. 4). In cases where the fracture did not cross the entire metaphyseal plane (*n* = 9 specimens), the medial aspect of the femur or tibia was most frequently involved (*n* = 5), regardless of the applied bending direction (varus in three, valgus in two) (Figs. 5 and 6). A classic metaphyseal lesion pattern was identified in only the central aspect of the femur or tibia in three cases (all varus) and the lateral aspect in one case (valgus). In two specimens, significant displacement of the femoral epiphyses was noted after testing (Fig. 4B).

In addition to the microcomputed tomography images, bending-moment-versus-time curves were reviewed for further evidence of fracture. Figure 7 shows the time histories for specimens with a classic metaphyseal lesion. In general, the time-history curves displayed two

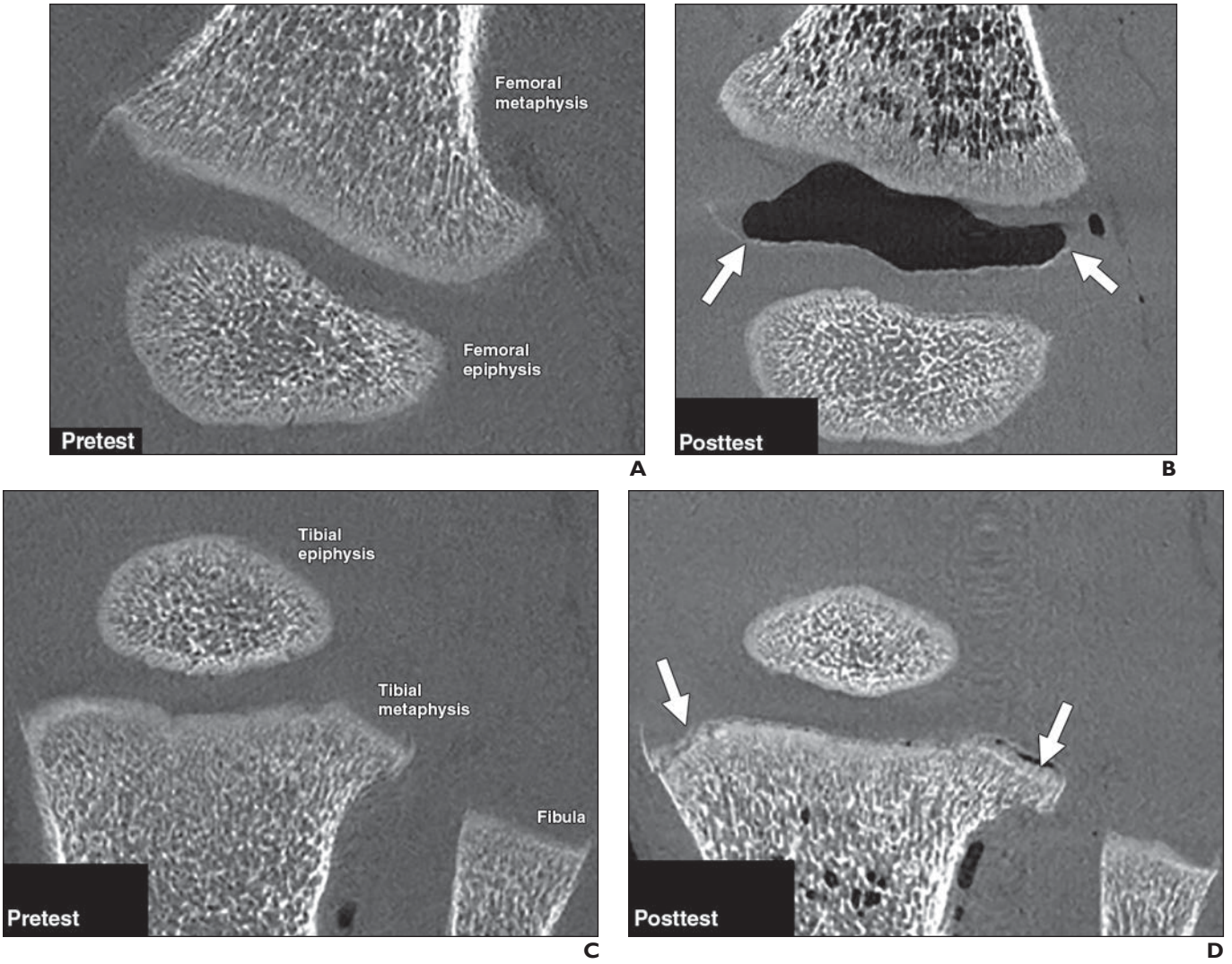

Fig. 4—Coronal microcomputed tomography images of 7-day-old specimen 3L. Specimen was tested in valgus bending with peak applied moment of 6.8 Nm.
A and **B,** Images of femur before (**A**) and after (**B**) testing are shown. Bony fragments separated from metaphysis indicate fracture (*arrows,* **B**).
C and **D,** Images of tibia before (**C**) and after (**D**) testing are shown. Bony fragments separated from metaphysis indicate fracture (*arrows,* **D**).

distinct regions: first, an initial "toe" region, in which applied moment was relatively constant (owing to laxity in the joint where displacement occurred at low levels of bending moment); and second, the primary loading curve, in which the bending moment increased nonlinearly. Rapid drops or decreases in the applied bending moment occurred in eight of the 12 specimens for which microcomputed tomography images revealed evidence of fracture (e.g., in Fig. 7A, there is a drop in moment for specimen 3L at 6.5 Nm). Bending-moment-versus-time plots showed no rapid decrease in bending moment during testing in the 4 remaining specimens (7-day-old specimens 5R, 6L, and 6R and 3-day-old specimen 16L) despite evidence of fracture in microcomputed tomography images. Conversely, sudden drops or decreases in bending moment were identified during testing of two specimens for which microcomputed tomography revealed no evidence of fracture. This suggests that the characteristic drop in bending moment may have been due to failure in tissue other than bone tissue or that image resolution was not adequate to detect bone tissue failure. As expected, bending moments necessary to generate fracture patterns consistent with classic metaphyseal lesions were lower than moments associated with the growth plate separation failure mechanism that occurred in our preliminary testing.

Discussion

In this study, metaphyseal fractures structurally consistent with clinical classic metaphyseal lesions were experimentally produced in immature porcine pelvic limbs through controlled varus and valgus bending. Previous studies have reported bending loading conditions as a mechanism that generated fractures resembling classic metaphyseal lesions [8–10]. In this study, we aimed to build on that work by applying bending loads in a controlled manner, measuring bending moments associated with fracture, and documenting the resulting fracture patterns using microcomputed tomography. Fractures were generated in both 3- and 7-day-old specimens in both varus and valgus bending. Lateral bending generates tensile forces on one side of the bone and compressive forces on the other (e.g., in valgus bending, bone tissue on the medial aspect will be under tension whereas bone tissue on the lateral aspect will be under

compression). Thus, it was expected that the fracture region would be dependent on the direction of loading (varus or valgus). However, both varus and valgus loading directions produced fractures on the medial aspect, lateral aspect, or both. The majority of fractures generated in this study traversed the entire plane of the metaphysis. However, when fractures did not traverse the entire metaphysis, the medial aspect of the femur or tibia was most often involved. This is consistent with clinical classic metaphyseal lesions of the distal femur and proximal tibia, which most often involve the posteromedial aspect [4, 5]. Kleinman and Marks [4, 5] hypothesized that the medial aspects of the distal femur and proximal tibia were weaker than the corresponding lateral aspects due to anatomic differences. Our findings of fractures primarily occurring in the posteromedial regions of the distal femur and proximal tibia, despite loading direction (varus vs. valgus), are likely due to these anatomical differences that result in weaker medial regions of the distal femur and proximal tibia. Reduced trabecular density at the medial aspect and discontinuity between the subperiosteal bone collar and cortex, as highlighted by Kleinman and Marks, would lead to higher trabecular stress in this region and, thus, the likely location of fracture initiation.

Specimens were loaded to peak bending moments ranging from 3.2 to 6.8 Nm that were applied dynamically at a rate of 42 mm/s. Fractures occurred at or below these peak moments, although exact fracture loads for each specimen could not be determined. The bending-moment-versus-time plots were reviewed for each specimen to determine whether any indication of fracture generation was evident. However, we determined that use of loading history plots alone was not sufficient to predict fracture given that plots for some specimens without fracture showed similar profiles (sudden decrease in moment) to those with fracture. Moreover, it was not possible to determine the cause of each sudden decrease in the moment-versus-time curves. In addition to indications of fracture, decreases could have resulted from soft-tissue failure, yielding of the tissue before failure (owing to the ductility of immature bone), or movement artifacts in the test fixtures. In an attempt to compare the peak moments in this study to published failure loads of pediatric bone, measurements of the bending strength of femoral cortical bone reported by Currey and Butler [19] were used to estimate associated bending moments.

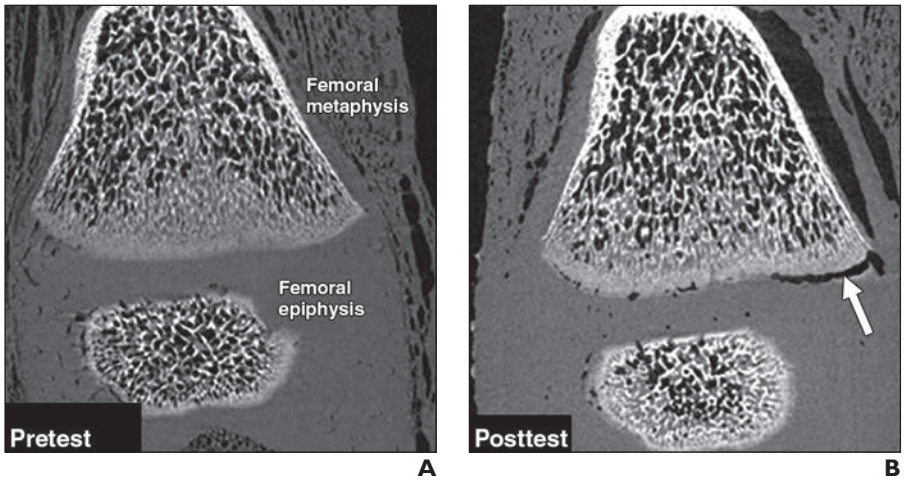

Fig. 5—Coronal microcomputed tomography images of 3-day-old specimen 15R. Specimen was tested in valgus bending with peak applied moment of 4.7 Nm.
A and **B,** Images of femur before (**A**) and after (**B**) testing are shown. Bony fragments separated from metaphysis indicate fracture (*arrow*).

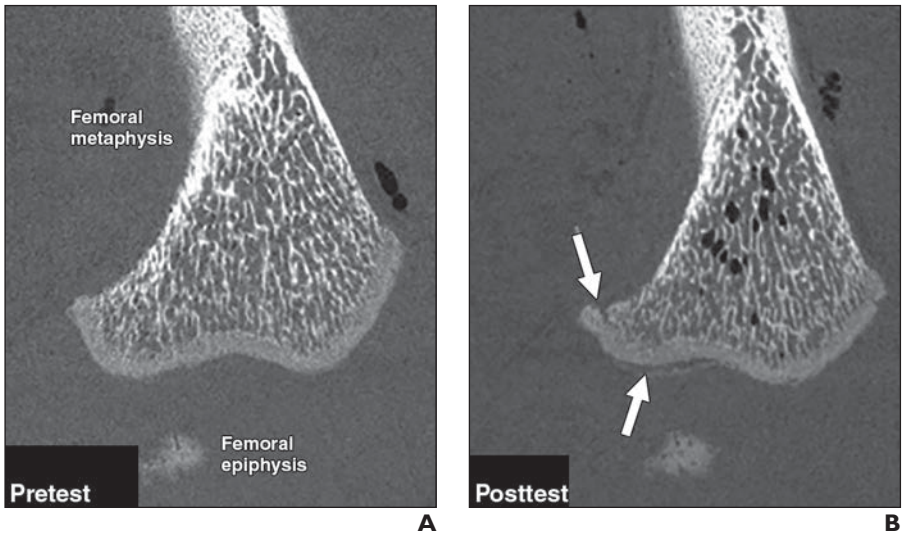

Fig. 6—Sagittal images of 3-day-old specimen 11L. Specimen was tested in valgus bending with peak applied moment of 3.2 Nm.
A and **B,** Images of femur before (**A**) and after (**B**) testing are shown. Bony fragments separated from metaphysis indicate fracture (*arrows,* **B**).

Using the provided dimensions of the Currey and Butler bone specimens, we estimated fracture bending moments of 1.2–1.4 Nm for children 2–4 years old. These loads are lower than peak bending moments applied in our study, in contrast to published findings that failure loads for cortical bone would be greater than metaphyseal trabecular bone [20]. However, Currey and Butler measured bending strength for small (2 mm thick) bone specimens (as opposed to whole bones) and applied bending loads quasi-statically (at a rate of 5 mm/min, which is much lower than the applied loading rate in our study). Because of the viscoelastic nature of bone, failure loads would likely be higher with increased loading rates. Additionally, our specimens included not only whole bones but also ligamentous structures having the ability to sustain a portion of loading. The maximum loading rate of our electromechanical testing machine was used in an attempt to better simulate real-world injury-causing events.

Although classic metaphyseal lesions have commonly been described radiographically and histologically [4, 5, 21], only one other study has documented the appearance of classic metaphyseal lesions using microcomputed tomography [22]. Because of the small

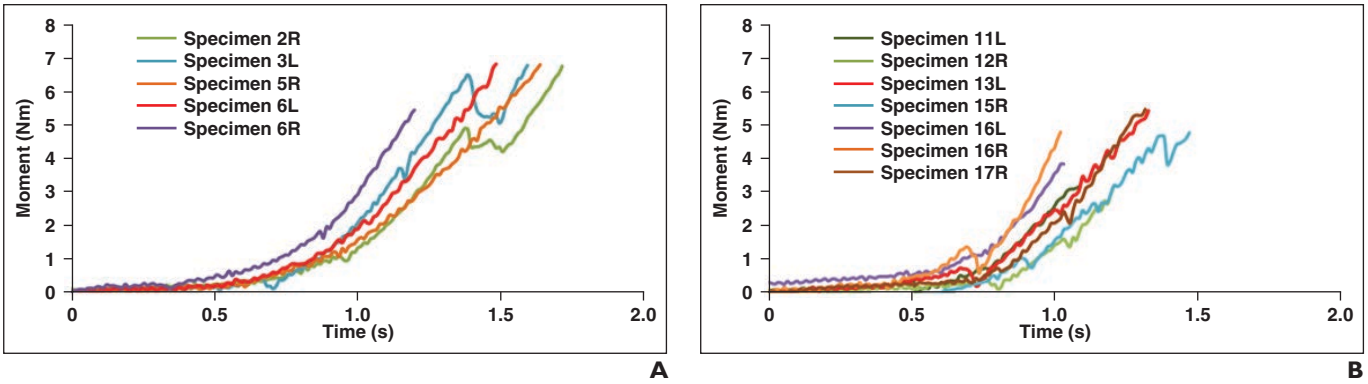

Fig. 7—Graphs plot applied bending moment versus time.
A and **B,** Curves show 7-day-old (**A**) and 3-day-old (**B**) porcine specimens with fracture patterns consistent with classic metaphyseal lesions (based on microcomputed tomography images).

size of the bone specimens in this study, microcomputed tomography was particularly useful to enable visualization of the trabecular structure. Tsai et al. [22] used high-resolution CT and histopathology to examine the morphology of normal metaphyseal bone in infants and that of infants with clinically diagnosed classic metaphyseal lesions, and this technique enabled them to examine the 3D morphology of the fracture in greater detail. Tsai et al. confirmed that classic metaphyseal lesions in infants are planar fractures through the metaphysis separating a mineralized bone fragment that is thin centrally and thicker peripherally where it encompasses the subperiosteal bone collar. In our study, classic metaphyseal lesion patterns had greater variation and did not always contain the thicker peripheral fragment. Additionally, clinical diagnosis of classic metaphyseal lesions is often aided by evidence of fracture healing (e.g., accumulation of hypertrophic chondrocytes at the fracture site), which was not possible in our in vitro study [4, 22].

Suggested causes of the classic metaphyseal lesion in infants include pulling or twisting a child's extremities or inertial forces generated by shaking an infant [3, 7, 22]. Reported accidental causes include birth trauma (e.g., breech birth) or clubfoot repair [6, 7]. Each of these mechanisms would likely include combinations of bending, torsion, and tensile forces. In this study, pure varus and valgus bending loads were found to generate metaphyseal fractures consistent with clinical classic metaphyseal lesions. It is possible that other loading mechanisms—such as tension and torsion, as well as combined loading such as that involved in yanking or twisting an infant's extremities—would also produce classic metaphyseal lesions. These loading mechanisms should be investigated further in future studies.

In the present study, metaphyseal fractures consistent with clinical classic metaphyseal lesions were replicated in an animal model under controlled loading. Our results indicate that classic metaphyseal lesions can result from a single loading event of lateral bending and that classic metaphyseal lesions are in fact fractures. Thus, we propose the term "classic metaphyseal fracture" be used in lieu of "classic metaphyseal lesion." A change in terminology may provide greater clarity because the term "lesion" is general, implying tissue damage for many reasons, and is not specific to trauma, whereas the term "fracture" is more precise, implying bone failure from trauma.

Limitations

One limitation of this study is the small sample size. Because of the small number of specimens, only one loading scenario was evaluated (pure bending), and we were not able to draw statistical conclusions regarding the influence of age or loading direction on probability of fracture. Future efforts are needed to evaluate whether other loading conditions (e.g., tension or torsional loads) or loading rates can generate similar fracture patterns. Another limitation is that bending tests were not performed in vivo. This prevented histologic confirmation, which often depends on the reaction or healing response to injury (e.g., reduced trabecular density, fibrosis) [3]. Specimens were frozen before testing. Freezing has been shown to affect the microstructure of bone evaluated histologically [23–25]. Studies have shown that freezing does not affect bone mechanical properties; however, these studies were conducted on adult (porcine and goat) bone tissue, and it is unclear whether the same holds true for the immature bone specimens used in this study [26, 27]. Additionally, because the stifle joint remained intact during testing, cartilage, ligaments, and other soft tissues were involved in transferring loading to the bone. It is possible that the mechanical properties of these tissues were affected by freezing. Structural and material property differences likely exist between immature porcine and human infant bones given developmental status and bipedal versus quadrupedal mobility at later stages of development. Thus, the bending moments associated with fracture measured in this study may not be directly applicable to human infants. The larger mass and differing bone morphology of human infants as compared with the immature piglets used in this study suggests that fracture moments would need to be scaled to account for these differences to translate our findings. Questions remain regarding the similarities and differences in structure and material properties between human and porcine infant bone and the potential translation of animal model findings to humans. Last, microcomputed tomography was useful in this study to visualize the fractures and trabecular structure at high resolution. However, it is possible that trabecular damage associated with classic metaphyseal lesions occurred but was not visually evident at the 20-μm resolution on all specimens. In future studies, histologic analysis should be included to examine the trabecular structure.

Conclusion

Metaphyseal fractures structurally consistent with clinical classic metaphyseal lesions were experimentally produced in immature porcine pelvic limbs through application of controlled varus and valgus bending. Pre- and posttest microcomputed tomography (at 20-μm resolution) was performed on specimens to identify the presence or absence of

fractures. Metaphyseal fractures occurred within peak applied bending moments ranging from 3.2 to 6.8 Nm. The majority of fractures appeared on the medial aspect of the bone, regardless of whether varus or valgus loading was applied. The results of this study indicate that classic metaphyseal lesions are fractures that can result from a single loading event and mechanistically support a change in terminology from classic metaphyseal lesion to classic metaphyseal fracture. Future work will involve development of a finite element computer model of an immature porcine femur to determine whether other loading conditions could produce a similar fracture.

References

1. Kleinman PK, Marks SC Jr, Richmond JM, Blackbourne BD. Inflicted skeletal injury: a postmortem radiologic-histopathologic study in 31 infants. *AJR* 1995; 165:647–650
2. Galleno H, Oppenheim WL. The battered child syndrome revisited. *Clin Orthop Relat Res* 1982; 162:11–19
3. Kleinman PK. Problems in the diagnosis of metaphyseal fractures. *Pediatr Radiol* 2008; 38(suppl 3):S388–S394
4. Kleinman PK, Marks SC Jr. A regional approach to the classic metaphyseal lesion in abused infants: the distal femur. *AJR* 1998; 170:43–47
5. Kleinman PK, Marks SC Jr. A regional approach to the classic metaphyseal lesion in abused infants: the proximal tibia. *AJR* 1996; 166:421–426
6. Offiah A, van Rijn RR, Perez-Rossello JM, Kleinman PK. Skeletal imaging of child abuse (nonaccidental injury). *Pediatr Radiol* 2009; 39:461–470
7. Kaczor K, Pierce MC. Abusive fractures. In: Jenny C, ed. *Child abuse and neglect: diagnosis, treatment, and evidence*. St. Louis, MO: Saunders, 2011:275–295
8. Ruess L, O'Connor SC, Quinn WJ, Medina LS, Wells CN, Anderson ML. An animal model for the classic metaphyseal lesion of child abuse. *Pediatr Radiol* 2003; 33:S112
9. Kleinman PL, Zurakowski D, Strauss KJ, et al. Detection of simulated inflicted metaphyseal fractures in a fetal pig model: image optimization and dose reduction with computed radiography. *Radiology* 2008; 247:381–390
10. O'Connor SC, Ruess L, Quinn WJ, Medina LS, Wells CN, Anderson ML. Film screen and computed radiography in the detection of classic metaphyseal lesions in an animal model of child abuse. *Pediatr Radiol* 2003; 33:S101
11. Shulman RJ. The piglet can be used to study the effects of parenteral and enteral nutrition on body composition. *J Nutr* 1993; 123:395–398
12. Koo WW, Hammami M, Hockman EM. Use of fan beam dual energy x-ray absorptiometry to measure body composition of piglets. *J Nutr* 2002; 132:1380–1383
13. Koo WW, Hammami M, Hockman EM. Validation of bone mass and body composition measurements in small subjects with pencil beam dual energy X-ray absorptiometry. *J Am Coll Nutr* 2004; 23:79–84
14. Koo MW, Yang KH, Begeman P, Hammami M, Koo WW. Prediction of bone strength in growing animals using noninvasive bone mass measurements. *Calcif Tissue Int* 2001; 68:230–234
15. Pierce MC, Valdevit A, Anderson L, Inoue N, Hauser DL. Biomechanical evaluation of dual-energy x-ray absorptiometry for predicting fracture loads of the infant femur for injury investigation: an in vitro porcine model. *J Orthop Trauma* 2000; 14:571–576
16. Cattaneo C, Marinelli E, Di Giancamillo A, et al. Sensitivity of autopsy and radiological examination in detecting bone fractures in an animal model: implications for the assessment of fatal child physical abuse. *Forensic Sci Int* 2006; 164:131–137
17. Bradley AL, Swain MV, Neil Waddell J, Das R, Athens J, Kieser JA. A comparison between rib fracture patterns in peri- and postmortem compressive injury in a piglet model. *J Mech Behav Biomed Mater* 2014; 33:67–75
18. Pyle SI, Hoerr NL. *A radiographic standard of reference for the growing knee*. Springfield, IL: Charles C. Thomas, 1969
19. Currey JD, Butler G. The mechanical properties of bone tissue in children. *J Bone Joint Surg Am* 1975; 57:810–814
20. Goldstein S, Frankenburg E, Kuhn J. Biomechanics of bone. In: Nahum A, Melvin J, eds. *Accidental injury: biomechanics and prevention*. New York, NY: Springer-Verlag, 1993:198–223
21. Kleinman PK, Marks SC, Blackbourne B. The metaphyseal lesion in abused infants: a radiologic-histopathologic study. *AJR* 1986; 146:895–905
22. Tsai A, McDonald AG, Rosenberg AE, Gupta R, Kleinman PK. High-resolution CT with histopathological correlates of the classic metaphyseal lesion of infant abuse. *Pediatr Radiol* 2014; 44:124–140
23. Tersigni MA. Frozen human bone: a microscopic investigation. *J Forensic Sci* 2007; 52:16–20
24. Lander SL, Brits D, Hosie M. The effects of freezing, boiling and degreasing on the microstructure of bone. *Homo* 2014; 65:131–142
25. Andrade MG, Sa CN, Marchionni AM, dos Santos Calmon de Bittencourt TC, Sadigursky M. Effects of freezing on bone histological morphology. *Cell Tissue Bank* 2008; 9:279–287
26. Matter HP, Garrel TV, Bilderbeek U, Mittelmeier W. Biomechanical examinations of cancellous bone concerning the influence of duration and temperature of cryopreservation. *J Biomed Mater Res* 2001; 55:40–44
27. van Haaren EH, van der Zwaard BC, van der Veen AJ, Heyligers IC, Wuisman PI, Smit TH. Effect of long-term preservation on the mechanical properties of cortical bone in goats. *Acta Orthop* 2008; 79:708–716